# Climatic and tectonic controls on weathering in south China and Indochina Peninsula: Clay mineralogical and geochemical investigations from the Pearl, Red, and Mekong drainage basins.

Z.F Liu, Christophe Colin, W. Huang, K.P Le, S.Q Tong, Z. Chen, A. Trenteseaux

Geochemistry Geophysics Geosystems G3
AN ELECTRONIC JOURNAL OF THE EARTH SCIENCES
Published by AGU and the Geochemical Society

*Article*
Volume 8, Number 5
11 May 2007
Q05005, doi:10.1029/2006GC001490
ISSN: 1525-2027

# Climatic and tectonic controls on weathering in south China and Indochina Peninsula: Clay mineralogical and geochemical investigations from the Pearl, Red, and Mekong drainage basins

**Zhifei Liu**
*State Key Laboratory of Marine Geology, Tongji University, Shanghai 200092, China (lzhifei@mail.tongji.edu.cn)*

**Christophe Colin**
*Laboratoire IDES, Bât. 504, UMR 8148 CNRS, Université de Paris XI, F-91405 Orsay, France*

**Wei Huang**
*State Key Laboratory of Marine Geology, Tongji University, Shanghai 200092, China*

**Khanh Phon Le**
*Oil and Gas Faculty, Hanoi University of Mining and Geology, Hanoi, Vietnam*

**Shengqi Tong**
*State Key Laboratory of Marine Geology, Tongji University, Shanghai 200092, China*

**Zhong Chen**
*South China Sea Institute of Oceanology, Chinese Academy of Sciences, Guangzhou 510301, China*

**Alain Trentesaux**
*UMR PBDS 8110 CNRS/USTL, FR 1818, Université de Lille I, F-59655 Villeneuve d'Ascq, France*

[1] Results of clay mineralogy, major element geochemistry, and Sr and Nd isotopes in 93 argillaceous samples collected from drainage basins of the Pearl, Red, and Mekong rivers reveal different degrees of chemical weathering in Southeast Asia despite similar climate conditions across these regions. The kaolinite/illite ratio, illite chemistry index, and illite crystallinity can be used as indicators of chemical weathering intensity. These mineralogical proxies combined with the $K_2O/(Na_2O + CaO)$ molar ratio, chemical index of alteration (CIA), and weathering trends observed from major element results indicate intensive silicate weathering in the Pearl River basin, moderate to intensive in the Mekong River basin, and moderate in the Red River basin. Although a significant modification of $\varepsilon$Nd(0) values in our riverine sediments during chemical weathering and transport is unlikely, $^{87}Sr/^{86}Sr$ ratios are controlled by various states of chemical weathering of high-Sr minerals such as plagioclase (rich in Na and Ca) with a linear decrease trend from the Pearl, Mekong, to Red river basins. Our results suggest that it is not the warm climate with heavy monsoon precipitation but tectonics playing the most significant role in controlling weathering and erosion processes in south China and Indochina Peninsula. Strong physical erosion caused by tectonic activities and river incision along the eastern margin of the Tibetan Plateau and along the Red River fault system is responsible for high contents of primary minerals in the lowlands of Red and Mekong river basins.

**Components:** 11,196 words, 11 figures, 1 table.

**Keywords:** clay minerals; major elements; chemical weathering; Pearl River; Red River; Mekong River.

**Index Terms:** 1039 Geochemistry: Alteration and weathering processes (3617); 3617 Mineralogy and Petrology: Alteration and weathering processes (1039); 1065 Geochemistry: Major and trace element geochemistry.

**Received** 23 September 2006; **Revised** 24 January 2007; **Accepted** 12 February 2007; **Published** 11 May 2007.

Liu, Z., C. Colin, W. Huang, K. P. Le, S. Tong, Z. Chen, and A. Trentesaux (2007), Climatic and tectonic controls on weathering in south China and Indochina Peninsula: Clay mineralogical and geochemical investigations from the Pearl, Red, and Mekong drainage basins, *Geochem. Geophys. Geosyst.*, *8*, Q05005, doi:10.1029/2006GC001490.

## 1. Introduction

[2] Evaluating factors controlling continental weathering and erosion is crucial for a better understanding of earth science processes [*Gaillardet et al.*, 1999; *Clift*, 2006]. Moreover, chemical and physical denudation of silicates can potentially affect the global carbon cycle and thereby global climate [*Raymo et al.*, 1988; *Raymo and Ruddiman*, 1992]. On various geological timescales, tectonic-driven mountain uplift, precipitation, and climate variability have been considered as the primary controlling factors on erosion, although their relative roles remain intensely debated [*Zhang et al.*, 2001; *Burbank et al.*, 2003; *Reiners et al.*, 2003; *Dadson et al.*, 2003; *Molnar*, 2004; *Clift et al.*, 2006a]. Such debate has further reinforced the need for a clearer understanding of the factors that control weathering and erosion occurring in mountain belts and world's largest river basins today [*Milliman and Syvitski*, 1992; *McLennan*, 1993; *Summerfield and Hulton*, 1994; *Canfield*, 1997; *Gaillardet et al.*, 1999; *Singh et al.*, 2005; *Selvaraj and Chen*, 2006].

[3] One area with weathering products particularly useful for evaluating the importance of climatic, tectonic, or erosional control on weathering and erosion is the region of Southeast Asia [*Clark et al.*, 2004; *Liu et al.*, 2005; *Clift et al.*, 2004]. Here continental scale strike-slip faults, extensive crustal thickening, surface uplift, and regional climatic interactions have shaped the dramatic modern landscape [*Schoenbohm et al.*, 2004; *Clift et al.*, 2006a, 2006b]. The fluvial systems have the highest denudation rates in the world [*McLennan*, 1993; *Summerfield and Hulton*, 1994] and supply as much as 70% of the global suspended sediment to the world ocean [*Milliman and Meade*, 1983]. Studies of weathering and erosion based on river geochemistry have been carried out in the Yangtze and Yellow rivers in North China, on the island of Taiwan, and in the Ganges-Brahmaputra River system in South Asia [*Zhang et al.*, 1990; *Galy and France-Lanord*, 1999; *Yang et al.*, 2004; *Singh et al.*, 2005; *Selvaraj and Chen*, 2006]. However, only a few studies have been conducted in the Pearl River in south China [*Zhang and Wang*, 2001], and almost none in the Red and Mekong rivers in Indochina Peninsula, though the region is unique for addressing uplift of the Tibetan Plateau, changes in land-sea patterns, and the reorganization of river networks [*Wang*, 2004; *Clift et al.*, 2006b].

[4] In this study, clay mineralogy, major element geochemistry, and Sr-Nd isotopes have been investigated for the first time on modern argillaceous sediments along the Pearl, Red, and Mekong rivers in order to evaluate the present weathering and erosion processes and their weathering mechanisms in the region. These three river basins now experience similar climate conditions but have been affected earlier by different tectonic activities apart from their geographic differences. To obtain information on sediment sources, Sr and Nd isotope compositions were analyzed. Sr and Nd isotope results were then combined with mineralogical (clay mineral content, illite chemistry index, and illite crystallinity) and major element (chemical index of alteration (CIA), $K_2O/(Na_2O + CaO)$ molar ratio) proxies to quantify chemical weathering states for the river sediments.

## 2. Hydrographic and Geological Settings

[5] The Pearl, Red, and Mekong drainage basins respectively run through south China and Indochina and all drain into the South China Sea (Figure 1). This region is dominated by the subtropical Asian monsoon climate, with an annual heavy rainfall of 1700–2000 mm (Figure 2)

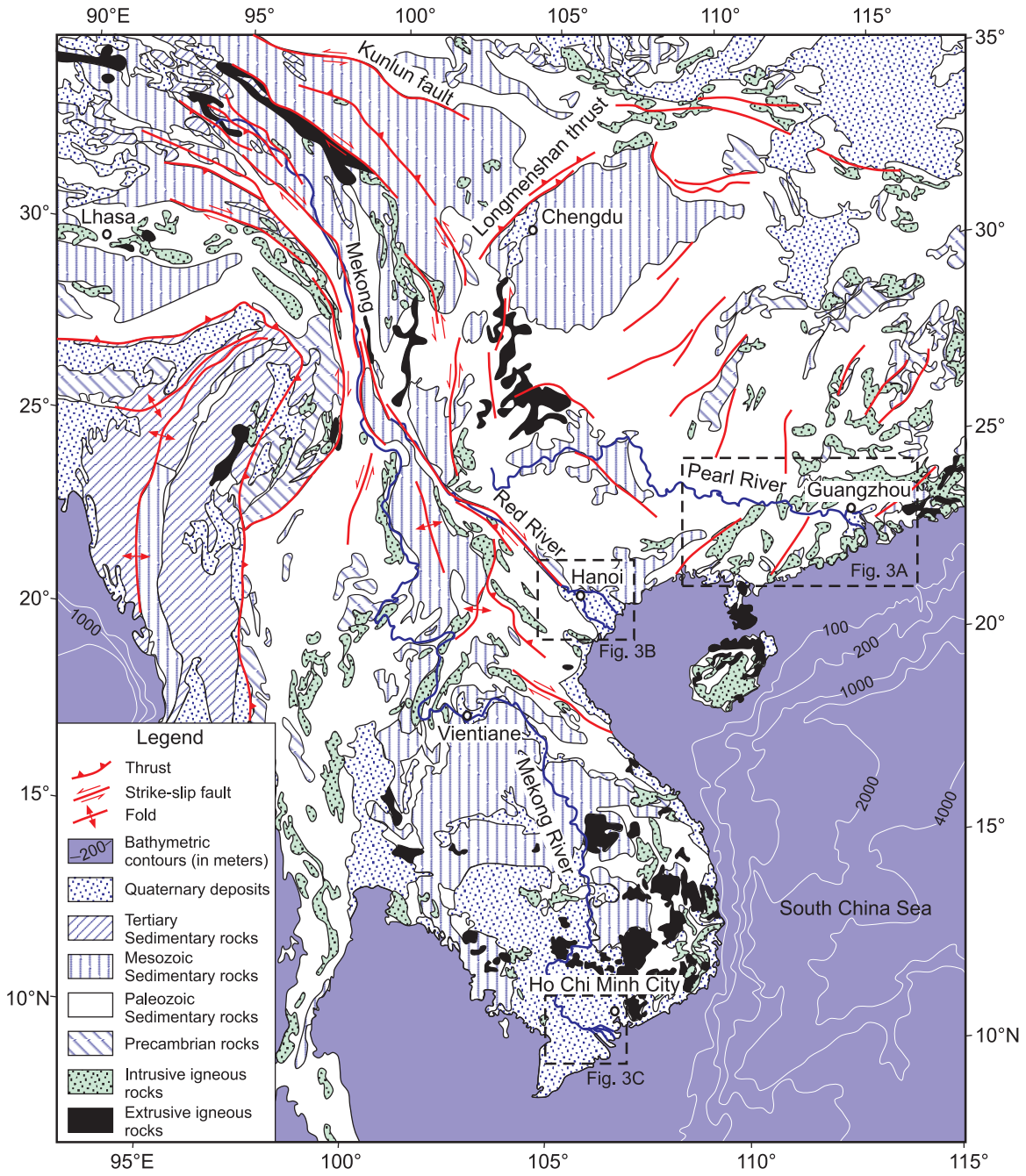


**Figure 1.** Geological map and bathymetry of SE Asia (modified after *Commission for the Geological Map of the World* [1975]) and locations of study areas (squared) in the Pearl, Red, and Mekong river basins. Bathymetry in meters.

[*Zhang and Wang*, 2001; *Gupta et al.*, 2002]. Rain everywhere is seasonal, with nearly 85–90% of the annual rainfall arriving during the summer monsoon season between May and October. However, the headwaters of the Mekong and Red rivers, which are situated in the eastern Tibetan Plateau, have a humid and cold climate during summer monsoon seasons, and parts of their discharges are derived from plateau's summer snowmelt. Temperature in Pearl and Red deltas varies between 13–30°C in winter and 16–29°C in summer, but the Mekong River delta has relatively uniform temperature range between 26 and 30°C, without obvious winter to summer difference (Figure 2). All the three rivers rank among the largest rivers in the world in terms of annual average sediment dis-

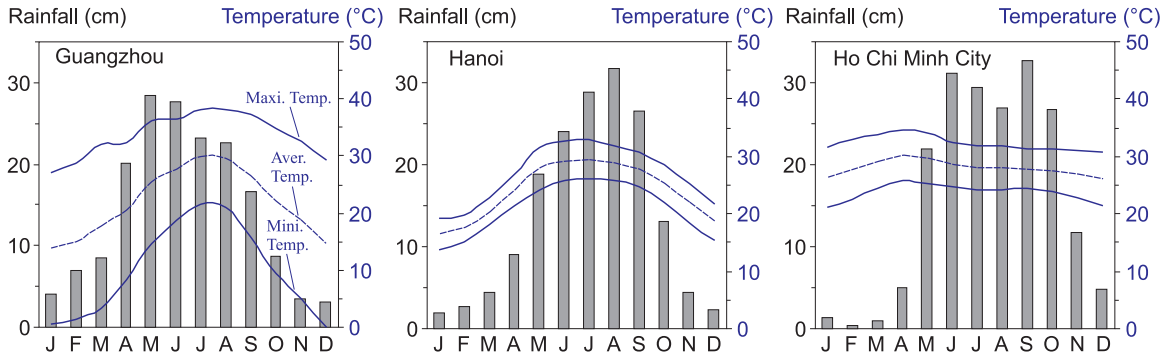


**Figure 2.** Rainfall and temperature distribution at stations of Guangzhou, Hanoi, and Ho Chi Minh City from lower reaches of the Pearl, Red, and Mekong river basins, respectively. See Figure 1 for the station locations. Monthly average data of Guangzhou between 1971 and 2000 are obtained online through the China Meteorological Data Sharing Services Network (http://cdc.cma.gov.cn); data of Hanoi (between 1898 and 1990) and Ho Chi Minh City (between 1906 and 1990) are from online data of the World Weather Information Service (http://www.worldweather.org/).

charge: 69 $\times$ $10^6$ t for the Pearl, 130 $\times$ $10^6$ t for the Red, and 160 $\times$ $10^6$ t for the Mekong [*Milliman and Meade*, 1983; *Milliman and Syvitski*, 1992]. The three river basins are well vegetated through all seasons except the highlands in Red and Mekong basins during winter. Average annual runoff is 686 mm for the Pearl, 1025 mm for the Red, and 595 mm for the Mekong [*Milliman and Meade*, 1983].

[6] Despite sharing similar East Asian monsoon climate and hydrologic conditions, the three river basins have quite different relief and geological settings. The Pearl River mostly drains through the low relief south China craton composed of Mesozoic-Cenozoic granite rocks and Paleozoic carbonates (Figure 1). The western part of the Pearl drainage basin is dominated by Paleozoic-Mesozoic carbonate rocks, mainly Permian-Triassic limestone; while in its eastern part, Mesozoic-Cenozoic granitic rocks and Paleozoic sedimentary rocks (limestone, shale, and sandstone) are the major rock types. The Red and Mekong rivers originate on a high relief of the Tibetan Plateau and flow southeastward through steep valleys along the eastern Tibetan margin into Indochina plains before meeting the South China Sea. The Red River flows along the NW-SE-aligned Red River fault system, which regulates the distribution of mountain areas, the drainage basin shape, and the river's relative straight course (Figure 1). Paleozoic-Mesozoic sedimentary rocks prevail in most parts of the upper and middle reaches, with minor intrusive and extrusive igneous rocks exposed along the Red River fault zone. Recent geomorphic and tectonic investigations revealed an active Red River fault even today [*Replumaz et al.*, 2001; *Leloup et al.*, 2001] and a minimum of 5 mm/yr long-term average slip rate since Pliocene time [*Schoenbohm et al.*, 2004, 2006a]. The Mekong River transects a major Paleozoic-Mesozoic sedimentary terrain (meta-sandstone, shale, slate, and phyllite), minor intrusive igneous rocks and Precambrian metamorphic rocks in its upper and middle reaches [*Liu et al.*, 2004, 2005], while Mesozoic sedimentary rocks (mainly sandstone and mudstone) prevail in most parts of the lower Mekong River basin, in which several large Neogene basalt bodies outcrop (Figure 1).

## 3. Sampling and Analytical Methods

[7] Fieldworks were carried out during dry seasons in March 2004 to the Pearl River and in January–February 2005 to the Red River and Mekong River in order to reach the river beds and collect muddy channel deposits. A set of 93 argillaceous samples (37 from the Pearl River basin, 39 from the Red River basin, and 17 from the Mekong River delta) were collected at 93 different locations (Figure 3). Sampling sites were chosen to avoid contamination from riverbank sediments. All samples were analyzed for clay minerals and major elements. Selected 20 samples with various geological settings and basin-wide distributions were also analyzed for Rb, Sr, and Nd concentrations, as well as for $^{87}Sr/^{86}Sr$ and $^{143}Nd/^{144}Nd$ ratios.

[8] Clay minerals were identified by X-ray diffraction (XRD) using a Philips PW 1710 diffractometer at the Laboratoire PBDS, Université de Lille I for Pearl River samples, and using a PANalytical

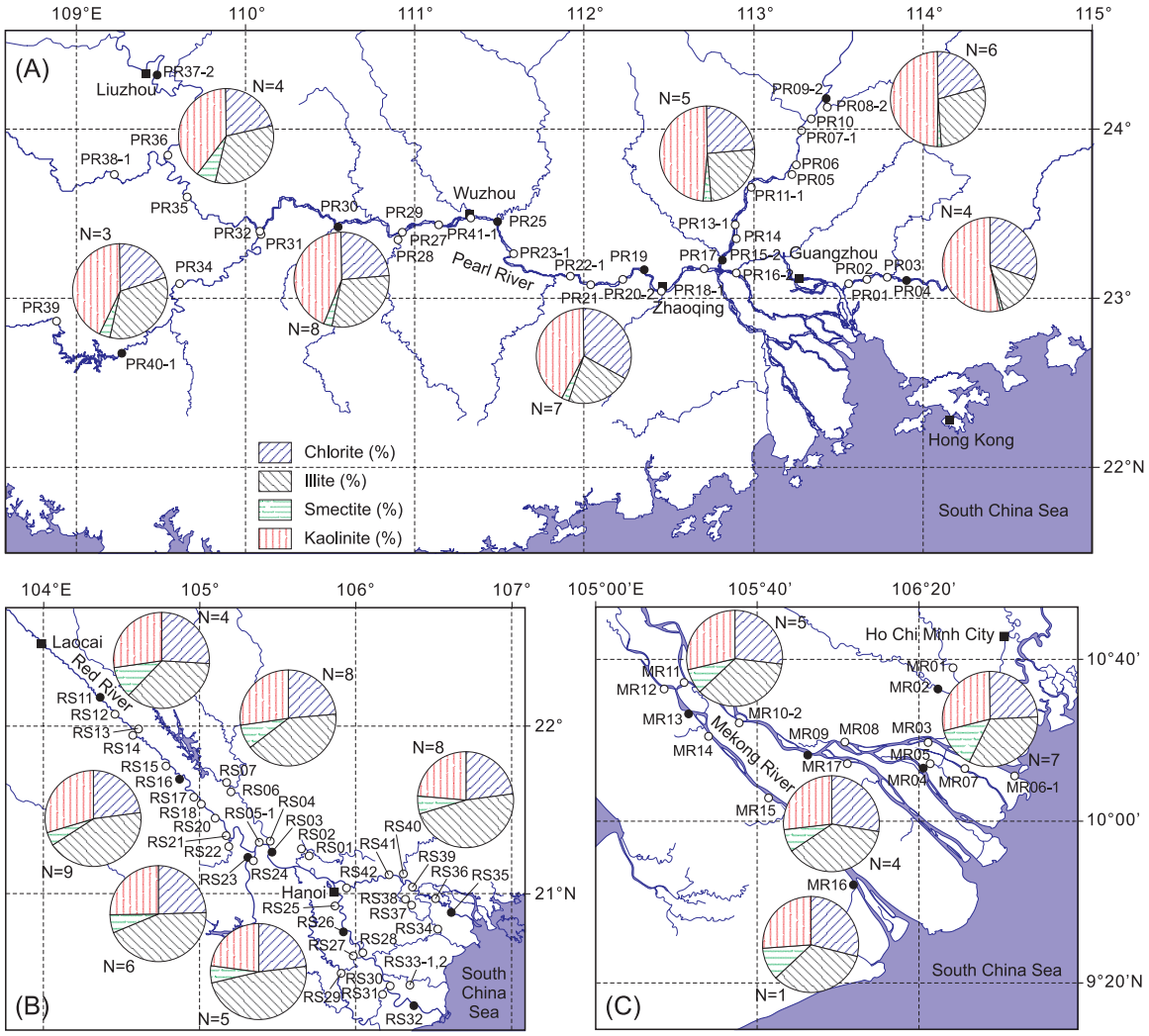


**Figure 3.** Sample locations and distribution of average clay mineral assemblages in the (a) Pearl River, (b) Red River, and (c) Mekong River drainage basins. See Figure 1 for their geographic locations and Table S1 for detailed GPS positions and clay mineral proportions. All samples were measured for clay minerals and major elements; selected samples with solid circles were also analyzed for Rb, Sr, and Nd concentrations and Sr-Nd isotopes. N, number of surface samples.

diffractometer at the Laboratoire IDES, Université de Paris XI for Red River and Mekong River samples on oriented mounts of non-calcareous clay-sized (<2 $\mu$m) particles [*Holtzapffel*, 1985]. The oriented mounts were obtained following the methods described in detail by *Liu et al.* [2004]. Several repeat samples analyzed by both laboratories show a difference less than the measuring accuracy (<5%) for each clay mineral concentration. Three XRD runs were performed, following air-drying, ethylene-glycol solvation for 24 hours, and heating at 520°C for two hours. Identification of clay minerals was made mainly according to the position of the (001) series of basal reflections on the three XRD diagrams. Semi-quantitative estimates of peak areas of the basal reflections for the main clay mineral groups of smectite (including mixed-layers) (15–17 Å), illite (10 Å), and kaolinite/chlorite (7 Å) were carried out on the glycolated curve [*Holtzapffel*, 1985] using the MacDiff software (available at http://servermac.geologie.uni-frankfurt.de/Staff/Homepages/Petschick/RainerE.html, 2001). Relative proportions of kaolinite and chlorite were determined on the basis of the ratio from the 3.57/3.54 Å peak areas.

[9] Geochemical analysis of major elements, Rb, Sr, and Nd concentrations, and Sr-Nd isotopes was performed on bulk carbonate- and organic-free sediments with particles <63 $\mu$m. Organic matter

and calcite were removed using 10% $H_2O_2$ and 1% HCl, respectively, in order to purify granule silicate particles. Particles <63 $\mu$m were wet sieved to remove potential local coarse grains that may significantly change the general geochemical composition. Our experiments indicate that there are almost no particles >63 $\mu$m in original argillaceous samples. XRD measurements on 40 calcite- and organic-free bulk samples (<63 $\mu$m) indicate that there is no significant content of dolomite in all river sediments. Major elements were measured by X-Ray fluorescence (XRF) using an ARL9800XP$^+$ spectrometer at the Center of Modern Analyses, Nanjing University. A mixture of 0.6000 g sample with 6.6000 g fluxing agent of Li tetraborate and Li metaborate ($Li_2B_4O_7$:$LiBO_2$ = 67:33) was added to a little 120 mg/l LiBr flux in a platinum crucible. The mixture was then fused using an automatic gas-fired CLAISSE burner system to make a glass disc for XRF measurement. The Rb, Sr, and Nd concentrations were analyzed by inductively coupled plasma-mass spectrometry (ICP-MS) using a Thermo VG-X7 mass spectrometer at the State Key Laboratory of Marine Geology, Tongji University. About 30–40 mg pre-prepared sediments were heated in an oven under 600°C. The sediments were then dissolved using a mixture solution of $HNO_3$ + HF on a hot plate. The eluted sample was diluted by 2% $HNO_3$ for the trace element measurement. Uncertainties on concentration measurement for Rb, Sr, and Nd are <3%.

[10] $^{87}Sr/^{86}Sr$ and $^{143}Nd/^{144}Nd$ isotopic ratios were measured using a thermal ionization Triton TI mass spectrometer at the State Key Laboratory for Mineral Deposits Research, Nanjing University. About 50 mg pre-prepared sediments were dissolved using a mixture solution of 2 mL concentrated HF and 0.5 mL concentrated $HNO_3$ under 120°C. Sr and Nd were eluted and purified following the methods described in detail by *Pu et al.* [2005]. The $^{87}Sr/^{86}Sr$ ratios have been corrected from mass fractionation using normalization to an $^{88}Sr/^{86}Sr$ ratio = 0.1194. Replicate analyses of NBS-987 Sr standard (n = 20) during the study gave a mean $^{87}Sr/^{86}Sr$ of 0.710260 ± 0.000010 (2$\sigma$), close to its certified value of 0.710250. Similarly, $^{143}Nd/^{144}Nd$ ratios have been corrected from mass fractionation using a normalization to the natural $^{146}Nd/^{144}Nd$ ratio = 0.7219. Replicate analyses of Nd JNdi standard (n = 15) during the study gave a mean $^{143}Nd/^{144}Nd$ of 0.512104 ± 0.000006 (2$\sigma$), close to its certified value of 0.512115. For convenience, Nd isotopic ratio results are expressed as $\varepsilon Nd(0) = [((^{143}Nd/^{144}Nd_{meas})/0.512638) - 1] \times 10000$, using the CHUR value given by *Jacobsen and Wasserburg* [1980].

## 4. Results

### 4.1. Clay Minerals

[11] For the clay fraction of the Pearl River sediments, kaolinite (30–67%) is the most dominant clay mineral with an average of 46%; chlorite (15–37%) and illite (6–40%) present in lesser abundance with a similar average content of about 25%. Smectite (0–11%) is very scarce with an average content of about 2% (auxiliary material Table S1).[1] Such results are in agreement with those obtained by *Boulay et al.* [2005] for a few Pearl River delta sediment samples. The clay mineral assemblages have been calculated for different river sections (Figure 3). Kaolinite is the dominant clay mineral, with more than 50% of the total clay content in the eastern part of the basin. Illite increases to about 10% of the total in the western part of the basin, but smectite is usually less than 2%, with an exception in the northwestern Pearl River where it forms about 10% of the sediment (Figure 3a). The illite chemistry index and illite crystallinity have been also calculated from the X-ray diffractograms. Illite chemistry index refers to the ratio of the 5 Å and 10 Å peak areas [*Esquevin*, 1969]. Illite crystallinity was obtained from half height width of the 10 Å peak [*Chamley*, 1989]. Illite chemistry index in the entire Pearl River drainage basin is usually between 0.50 and 0.80, with only a few locations where values reach 0.45–0.50, and illite crystallinity varies between 0.24 and 0.42°$\Delta 2\theta$, with an average value of 0.30°$\Delta 2\theta$ (Table S1).

[12] For the Red River sediments, illite (31–57%) is the dominant clay mineral, with an average content of 44%; kaolinite (17–38%) and chlorite (6–29%) are less abundant, with a similar average content of about 25%; smectite (1–14%) is still a minor component averaging at 6%, and thus higher than in the Pearl River basin (Table S1). The clay mineral assemblages for different river sections display a similar distribution with a little higher smectite content in the upper reach (Figure 3b). The illite chemistry index varies between 0.27 and 0.63, but most of analyses are less than 0.50, with an average value of 0.40, and the illite crystallinity

[1] Auxiliary materials are available at ftp://ftp.agu.org/apend/gc/2006gc001490.

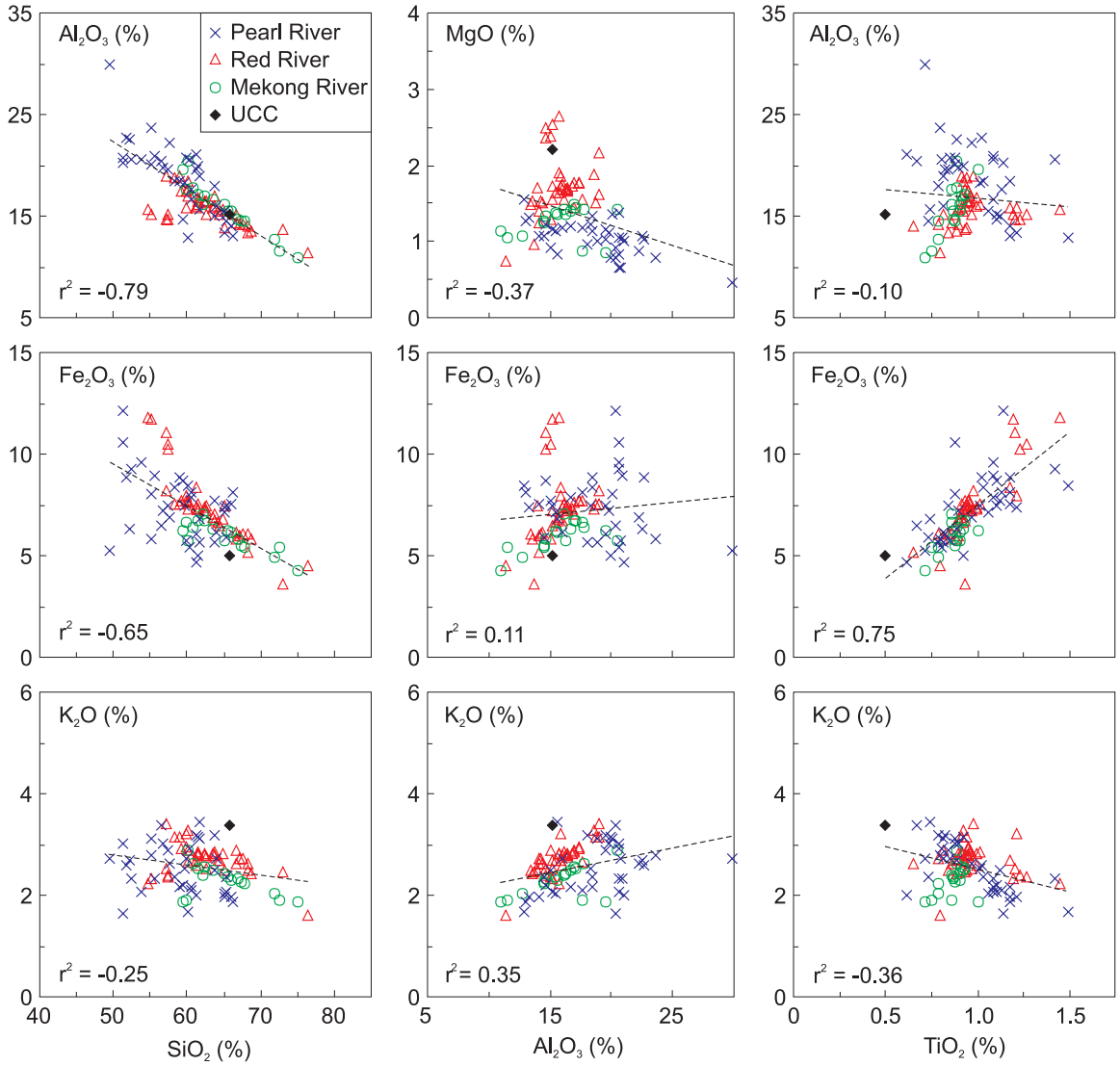


**Figure 4.** Selected variation diagrams of major elements in the Pearl, Red, and Mekong river basins are plotted against $SiO_2$, $Al_2O_3$, and $TiO_2$. Data of upper continental crust (UCC) from *Taylor and McLennan* [1985] were also plotted as a reference. Dashed lines indicate linear correlations with a coefficient ($r^2$).

is between 0.11 and 0.23°$\Delta 2\theta$, with an average value of 0.20°$\Delta 2\theta$ (Table S1).

[13] Samples from the Mekong River delta have similar clay mineral assemblages between various locations: kaolinite (24–41%), illite (21–38%), and chlorite (21–30%) again making up the dominant clay minerals with an average content of 28%, 35%, and 26%, respectively. Smectite (6–18%) is a minor clay mineral with an average percentage of 11%, a value considerably higher than the Pearl and Red records (Figure 3c). The illite chemistry index and illite crystallinity range between 0.46–0.90 and 0.19–0.21°$\Delta 2\theta$, respectively, with average values of 0.47 and 0.20°$\Delta 2\theta$ (Table S1).

## 4.2. Major Elements

[14] The bulk carbonate-free surface sediments (<63 $\mu$m) from the Pearl, Red, and Mekong basins are characterized by high contents of $SiO_2$, $Al_2O_3$, $Fe_2O_3$, and $K_2O$, and by low concentrations of MgO, $TiO_2$, CaO, $Na_2O$, $P_2O_5$, and MnO (Table S1). We have selected some elements and plotted them on variation diagrams using $SiO_2$, $Al_2O_3$, and $TiO_2$ along the $x$ axis (Figure 4). Data of upper continental crust (UCC) from *Taylor and McLennan* [1985] were also plotted as a reference. A moderate

**Table 1.** Rb, Sr, and Nd Concentrations and Sr-Nd Isotopic Data of Argillaceous Sediments From the Pearl River, Red River, and Mekong River[a]

| Sample | Sr, ppm | Rb, ppm | Nd, ppm | Rb/Sr | $^{87}Sr/^{86}Sr$ | Error | $^{143}Nd/^{144}Nd$ | Error | $\varepsilon Nd(0)$ | Error |
|---|---|---|---|---|---|---|---|---|---|---|
| PR04 | 52.6 | 207.2 | 50.9 | 3.94 | 0.733442 | 0.000003 | 0.512039 | 0.000041 | −11.7 | 0.80 |
| PR09-2 | 58.7 | 243.9 | 45.8 | 4.16 | 0.742222 | 0.000005 | 0.511957 | 0.000006 | −13.3 | 0.12 |
| PR15-2 | 62.1 | 235.6 | 49.5 | 3.79 | 0.735662 | 0.000006 | 0.511989 | 0.000005 | −12.7 | 0.10 |
| PR19 | 40.7 | 124.1 | 34.3 | 3.05 | 0.735209 | 0.000003 | 0.512106 | 0.000009 | −10.4 | 0.18 |
| PR25 | 71.9 | 128.6 | 49.8 | 1.79 | 0.727507 | 0.000002 | 0.512004 | 0.000003 | −12.4 | 0.06 |
| PR30 | 79.1 | 150.5 | 45.6 | 1.90 | 0.730134 | 0.000003 | 0.512053 | 0.000009 | −11.4 | 0.18 |
| PR37-2 | 64.1 | 171.9 | 63.0 | 2.68 | 0.737314 | 0.000005 | 0.512099 | 0.000029 | −10.5 | 0.57 |
| PR40-1 | 65.6 | 153.1 | 48.4 | 2.33 | 0.728329 | 0.000002 | 0.512025 | 0.000003 | −12.0 | 0.06 |
| RS03 | 150.1 | 64.9 | 34.1 | 0.43 | 0.734244 | 0.000004 | 0.512003 | 0.000004 | −12.4 | 0.08 |
| RS11 | 137.4 | 147.6 | 56.2 | 1.07 | 0.715813 | 0.000003 | 0.511968 | 0.000004 | −13.1 | 0.08 |
| RS16 | 151.2 | 146.2 | 58.6 | 0.97 | 0.717309 | 0.000003 | 0.512039 | 0.000004 | −11.7 | 0.08 |
| RS23 | 136.2 | 89.3 | 31.5 | 0.66 | 0.723133 | 0.000003 | 0.512106 | 0.000006 | −10.4 | 0.12 |
| RS26 | 144.9 | 92.5 | 42.3 | 0.64 | 0.725997 | 0.000003 | 0.512027 | 0.000006 | −11.9 | 0.12 |
| RS32 | 152.8 | 94.4 | 44.6 | 0.62 | 0.724829 | 0.000005 | 0.512050 | 0.000003 | −11.5 | 0.06 |
| RS35 | 152.6 | 87.8 | 39.0 | 0.58 | 0.727307 | 0.000003 | 0.512027 | 0.000005 | −11.9 | 0.10 |
| MR02 | 69.3 | 129.5 | 32.7 | 1.87 | 0.720276 | 0.000003 | 0.512131 | 0.000005 | −9.9 | 0.10 |
| MR04 | 94.3 | 146.3 | 31.1 | 1.55 | 0.720699 | 0.000002 | 0.512115 | 0.000004 | −10.2 | 0.08 |
| MR09 | 87.1 | 127.0 | 37.9 | 1.46 | 0.721307 | 0.000003 | 0.512082 | 0.000005 | −10.8 | 0.10 |
| MR13 | 88.7 | 140.6 | 39.0 | 1.58 | 0.722173 | 0.000003 | 0.512104 | 0.000005 | −10.4 | 0.10 |
| MR16 | 83.4 | 131.5 | 34.7 | 1.58 | 0.721801 | 0.000003 | 0.512098 | 0.000005 | −10.5 | 0.10 |

[a] PR, Pearl River; RS, Red River; MR, Mekong River. The samples were decarbonated and wet sieved (63 $\mu$m) before chemical analyses.

to strong negative correlation between $SiO_2$ and $Al_2O_3$ and $Fe_2O_3$ indicates potential grain-size control on $SiO_2$ content because quartz-rich mineral associations often produce a higher $SiO_2$ concentration. There is a great dispersion in diagrams of $K_2O$ versus $SiO_2$ and $Al_2O_3$. $K_2O/Al_2O_3$ ratios are low in smectite and kaolinite, and high in minerals such as illite, muscovite, and biotite. Ratios of $K_2O/SiO_2$ and $K_2O/Al_2O_3$ are high in Red River sediments, moderate in Mekong River sediments, and low in Pearl River sediments. The increasing trend of $TiO_2$ with $Fe_2O_3$ can be attributed to their common source from ferromagnesium minerals such as biotite, amphibole, and pyroxene. The major element results imply significant differences in mineralogical compositions between the three rivers.

### 4.3. Isotopic Results

[15] Rb, Sr, and Nd concentrations as well as $^{87}Sr/^{86}Sr$ ratios and $\varepsilon Nd(0)$ measured on carbonate-free fractions (<63 $\mu$m) are listed in Table 1. The Sr concentrations vary between 40.7–79.1 ppm for the Pearl River sediments, 136.2–152.8 ppm for the Red River, and 69.3–94.3 ppm for the Mekong River. The Rb concentrations show an opposite trend: 124.1–243.9 ppm for the Pearl, 64.9–147.6 ppm for the Red, and 127.0–146.3 ppm for the Mekong. Consequently, Pearl River sediments are characterized by higher Rb/Sr ratios than those of the Red and Mekong rivers.

[16] Mekong River sediments present narrow ranges of Sr-Nd isotopic values: $^{87}Sr/^{86}Sr$ ratios between 0.720 and 0.722 and $\varepsilon Nd(0)$ between −9.9 and −10.8. The Pearl and Red river sediments have similar, relative wider ranges of $\varepsilon Nd(0)$ between −10.4 and −13.3 and wider variations in $^{87}Sr/^{86}Sr$ ratios: 0.728–0.742 for the Pearl and 0.716–0.734 for the Red.

## 5. Discussion

### 5.1. Mineralogical Changes

[17] Significant different clay mineral assemblages exist in surface sediments from Pearl, Red, and Mekong drainage basins, as shown by the illite+chlorite – kaolinite – smectite ternary diagrams (Figure 5). Apparently, the differences in clay mineral distribution are related to the intensity of weathering, geology and weathering regime of the drainage basins [*Chen*, 1978; *Gingele et al.*, 2001].

[18] In general, weathering intensity is mainly controlled by lithology, climate, and morphology and, in turn, determines the formation of clays [*Chamley*, 1989]. A simple scenario is that parent rocks with different lithological compositions in

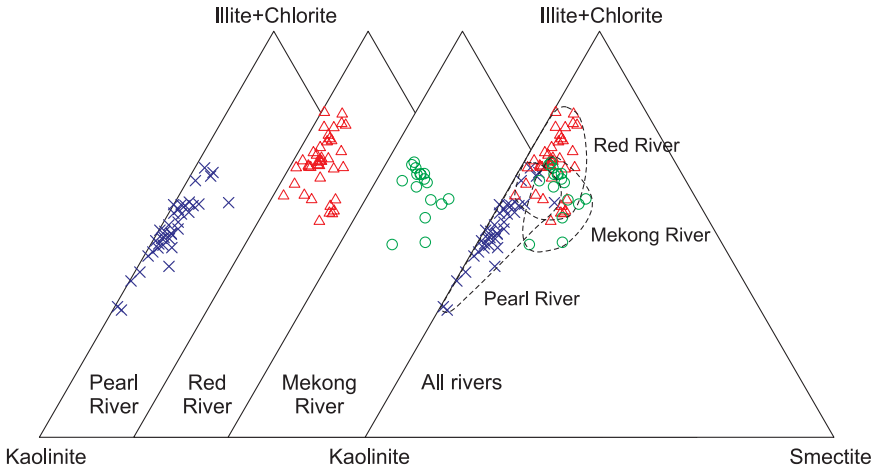


**Figure 5.** Comparison between clay mineral ternary diagrams of argillaceous sediments from the Pearl, Red, and Mekong basins.

the upper reach of a river attribute to various clay mineral distributions in its lower drainage basin. This scenario, however, does not apply to the Pearl, Red, and Mekong drainage basins. Although a large dissimilarity in their parent lithologies exists in each river basin, the clay mineral assemblage is similar basin-wide (Figures 3 and 5), implying a primary influence of hydrolytic conditions and morphology on clay formation. The reason for this basin-wide clay similarity appears to be upon the various hydrolytic weathering processes occurring in each river basin. During chemical weathering, subtraction of ions from minerals in parent rocks statistically concerns first the more mobile ions, like Na, K, Ca, Mg, and Sr. This hydrolytic weathering process has been called bisialitization with the formation of 2:1 layer clays (the assemblage of two tetrahedral sheets with one octahedral sheet, e.g., smectite) [*Pédro*, 1981]. Transitional elements tend to be evacuated later (Mn, Ni, Cu, Co, Fe), and followed by Si. This process corresponds to monosialitization with the formation of 1:1 layer clays (the assemblage of one tetrahedral sheet with one octahedral sheet, e.g., kaolinite). Al is the less mobile element through the hydrolytic process. The final process of hydrolytic weathering is alitization with the formation of Al hydroxides (e.g., gibbsite). An increase of hydrolysis intensity and ionic subtraction in weathering parent rocks gives way to secondary minerals that become more and more depleted in cations, especially the more mobile cations.

[19] Kaolinite is readily found in monosialitic soils, and therefore displays a strong climatic dependence controlled mainly by the intensity of continental hydrolysis [*Chamley*, 1989]. Kaolinite is also common on steep slopes within a drainage basin with relative good drainage conditions. There is much more kaolinite in the Pearl River sediments than in the sediments of two other rivers. Warm and humid climate conditions combined with a low-relief, stable (cratonic) morphology in the Pearl River basin encourage significant chemical weathering processes of monosialitization and alitization. Both granites in the east as well as sedimentary rocks in the entire basin produce a significant amount of kaolinite in modern clay mineral assemblages. Parent aluminosilicates associated with calcite and dolomite in the carbonate rocks in the west have undergone weathering processes similar to granitic and other sedimentary rocks in the eastern part of the Pearl River basin.

[20] Illite is the most abundant clay mineral in the Red and Mekong drainage basins with at least 35% of the total clay assemblage compared to the Pearl River sediments (Figure 3). Illite is considered as a primary mineral, which reflects decreased hydrolytic processes in continental weathering and increased direct rock erosion under cold and arid climatic conditions. In our three river basins, illite could have been derived from physical erosion of metamorphic and granitic parent rocks, mainly located at high elevation in eastern Tibet. Or it may have been formed by weathering of nonlayer silicate, such as feldspar from granites under moderate hydrolysis conditions, and by degradation of micas. Such illite formations occur mainly in the highland part of the Red and Mekong drainage basins, the eastern Tibetan Plateau and its marginal regions. Although warm and humid climate con-

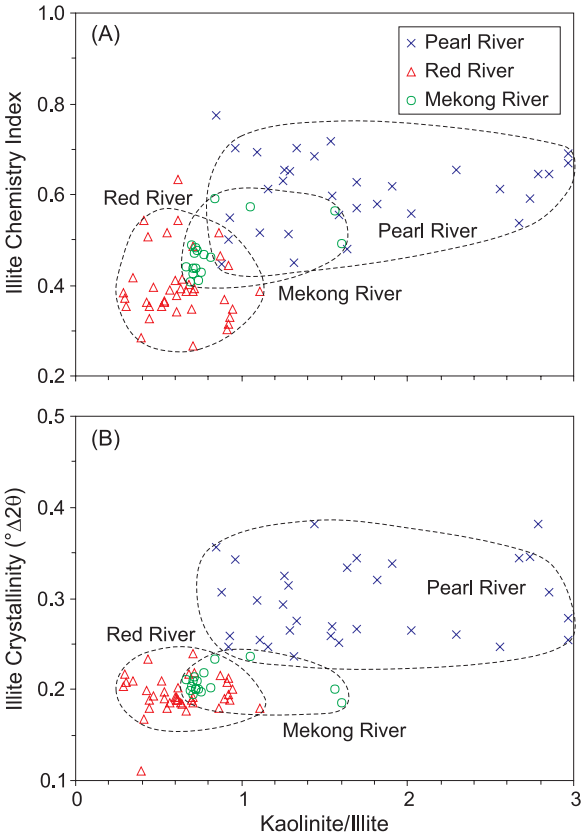


**Figure 6.** Correlations of kaolinite/illite ratio with (a) illite chemistry index and (b) illite crystallinity in argillaceous sediments from the Pearl, Red, and Mekong river basins.

ditions in their middle-lower reaches are similar to the Pearl River basin, the Red and Mekong river basins have a different history of tectonic activities and river incision in the eastern Tibetan Plateau and its marginal regions as well as humid and cold climate in their headwaters, which may have significantly increased physical erosion and decreased hydrolytic weathering processes as bisialitization and monosialitization. These weathering processes produce the high content of illite (primary mineral) and reasonable amount of kaolinite and smectite (secondary minerals) as found in samples analyzed. Mesozoic-Cenozoic sedimentary rocks prevail in the headwaters of the Mekong River basin in the Tibetan Plateau, allowing physical weathering processes to form lithosols containing only illite and chlorite [*Liu et al.*, 2003].

[21] Smectite is a secondary mineral, which is derived from chemical weathering of parent aluminosilicate and ferromagnesian silicate under warm and humid conditions. Smectite is formed in confined environments, by recombination of released cations. Smectite is not formed in the same part of the river basin as kaolinite. In the Mekong drainage basin, widely distributed bisiallitic soil in the middle and lower reaches is a potential source for smectite in the delta [*Liu et al.*, 2004]. Mineralogical components of the bisiallitic soil are 2:1 layer clays (e.g., smectite). Distribution of bisiallitic soil in the Pearl and Red river basins, however, is very limited [*Ségalen*, 1995]. Although the chemical weathering of extrusive basaltic rocks in various climatic conditions could produce smectite [*Griffin et al.*, 1968], the minor extrusive igneous rocks exposed along the Red River fault zone and several large Neogene basalt bodies outcropped in the lower Mekong River basin do not produce a significant amount of smectite, as indicated from the results of clay mineral assemblages of the Red and Mekong rivers (Figures 3b and 3c).

[22] Therefore the similar clay mineral assemblages basin-wide in each of these river basins suggest that the difference in clay mineral distribution in the Pearl, Red, and Mekong rivers can be attributed to the intensity of chemical weathering, tectonic activities, and tectonic-induced river incision, rather than their dissimilarity in parent lithology. The kaolinite/illite ratio hence can be used as a chemical weathering indicator. This mineralogical ratio is also independent from the weathering of volcanic rocks. Higher kaolinite/illite values indicate strengthened chemical weathering and weak physical erosion, and vice versa when the ratio is low.

[23] If considering that there is no important diagenesis or reworking for illite in all surface river samples, we can select illite chemistry index and illite crystallinity as indicators of the intensity of chemical weathering. Ratios of illite chemistry index lower than 0.5 represent Fe-Mg-rich illites, which are characteristic of weak chemical weathering conditions; ratios higher than 0.5 are found in Al-rich illites, which are formed by strong hydrolysis [*Esquevin*, 1969]. Lower values of illite crystallinity represent higher crystallinity, which is characteristic of weak hydrolysis in continental sources [*Chamley*, 1989; *Krumm and Buggisch*, 1991]. The high illite crystallinity may also require some degree of low temperature burial metamorphism as well. Our results, however, show highest illite crystallinity in the Red River basin with similar values for both metamorphic and sedimentary sources, and thus do not support the above

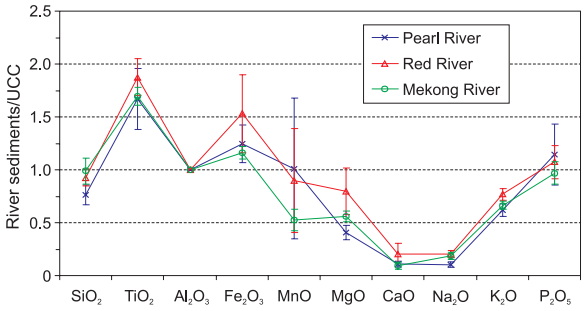


**Figure 7.** Elemental ratios of argillaceous sediments in the Pearl, Red, and Mekong river basins, calculated from average major element concentrations normalized to UCC [*Taylor and McLennan*, 1985] with respect to $Al_2O_3$. The error bar of each element refers to the standard deviation of all samples.

mentioned hypothesis. The kaolinite/illite ratio indicator fits well with the mineralogical results of illite chemistry index and illite crystallinity (Figure 6). Increase in the illite chemistry index, or decrease in the illite crystallinity (with higher values), is associated with an increased kaolinite/illite ratio, suggesting that these three mineralogical parameters indicate the average state of chemical weathering for the river sediments. Their values are high in the Pearl River sediments, moderate in the Mekong River sediments, and low in the Red River sediments. These results suggest that strengthened chemical weathering and strong hydrolysis operate in the Pearl River basin, moderate chemical weathering and moderate hydrolysis in the Mekong River basin, and relatively weak hydrolysis and strong physical erosion in the Red River basin.

## 5.2. Chemical Mobility and Weathering Trends

[24] Major element composition of river sediments can be used to assess the state of chemical and physical weathering and to determine the geochemical process operating in a river basin [*Vital and Stattegger*, 2000; *Singh et al.*, 2005]. The chemical composition of weathering products in a river basin is expected to demonstrate well-established concepts on mobility of various elements during weathering [*Nesbitt et al.*, 1980; *Singh et al.*, 2005]. We use elemental ratios calculated with respect to the least mobile element Al to identify and evaluate the major element mobility. The ratio of the content of element X and $Al_2O_3$ in river samples divided by the ratio of the same element content in UCC gives the following elemental ratio [*Singh et al.*, 2005]:

$$\text{Elemental ratio(X)} = \frac{X/Al_2O_3(rivers)}{X/Al_2O_3(UCC)}.$$

This elemental ratio refers to the relative enrichment or depletion of the element, i.e., >1 indicates enrichment, <1 indicates depletion, and = 1 indicates no change in the relative abundance of the element.

[25] The elemental ratios calculated from average major element concentrations normalized to UCC are displayed in Figure 7. All major elements from our three rivers show a similar chemical mobility with little differences. The mobility of $SiO_2$ is critical for understanding of chemical weathering. The $SiO_2$ content is depleted in the Pearl River sediments but rather stable in the Red and Mekong rivers, suggesting stronger chemical weathering occurring in the Pearl River basin. The immobile Ti is markedly enriched in all river sediments and, along with higher Fe values, it confirms their common source from ferromagnesium minerals in each individual river (Figure 4). The highly mobile elements Ca and Na from all the three rivers show similar lowest values related to their chemical weathering. Mg and K have become tightly incorporated in clay minerals, with more Mg in illite and more K in micaceous minerals. In comparison, more depleted Mg and K in Pearl River sediments suggest stronger chemical weathering than in the Red and Mekong river basins.

[26] The degree of chemical weathering can be estimated by the chemical index of alteration (CIA) [*Nesbitt and Young*, 1982]:

$$\text{CIA} = [Al_2O_3/(Al_2O_3 + \text{CaO}^* + Na_2O + K_2O)] \times 100,$$

where CaO* represents CaO associated with the silicate fraction of the sample. For primary minerals (non altered minerals), all feldspars have CIA value of 50 and the mafic minerals biotite, hornblende, and pyroxenes have CIA values between of 50–55, 10–30, and 0–10, respectively. Feldspar and mica weathering to smectite and kaolinite result in a net loss of K and Na in weathering profiles, whereas Al is resistant and is enriched in weathering products [*Nesbitt and Young*, 1982]. This induces an increase of CIA values by about 100 for kaolinite and 70–85 for smectite. The CIA value is thought to quantify the state of chemical weathering of the rocks by referring to the loss of labile elements such as Na,

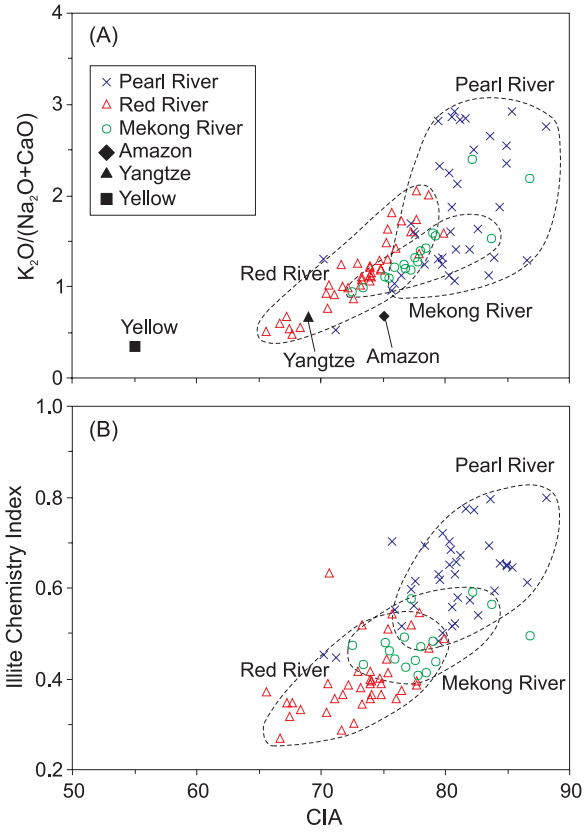


**Figure 8.** Correlations of chemical index of alteration (CIA) with (a) $K_2O/(Na_2O+CaO)$ molar ratio and (b) illite chemistry index of argillaceous sediments in the Pearl, Red, and Mekong river basins. The graphs show linear correlations of mineralogical and element geochemical proxies of chemical weathering. Average data of clayey sediments from the Amazon River [*Vital and Stattegger*, 2000], the Yellow River, and the Yangtze River [*Yang et al.*, 2004] were plotted for comparison.

Ca, and K. CIA values are 75–88 for the Pearl River sediments, 72–83 for the Mekong River sediments, and 65–78 for the Red River sediments (Figure 8). Such CIA values are in agreement with the clay mineralogical results, which indicate higher kaolinite/illite ratio for the Pearl River sediments and lower values for the Red River sediments (Figure 6).

[27] The CIA values are well correlated with the $K_2O/(Na_2O + CaO)$ molar ratio (Figure 8a) from the three rivers. The range of the $K_2O/(Na_2O + CaO)$ molar ratio in the three rivers strongly suggests changes of the mineralogy between an end-member rich in plagioclase (high content of Na and Ca) and another rich in K-feldspar, micas, and illite. Increase in the $K_2O/(Na_2O + CaO)$ molar ratio is associated with CIA increase, suggesting a preferential hydrolysis of plagioclase (enrichment of Na) relative to K-feldspar and micas (enrichment in K) during the silicate weathering process of river sediments. The much higher mobility in elements Ca and Na than in element K from all the three river basins (Figure 7) and more plagioclase in Red and Mekong river samples than in Pearl River samples by bulk XRD results support this hypothesis. A linear correlation of CIA with the illite chemical index (Figure 8b) also well demonstrate that the degree of chemical weathering is strongest in the Pearl River basin, moderate in the Mekong River basin, and relatively weak in the Red River basin. In comparison, chemical weathering in the Amazon River [*Vital and Stattegger*, 2000], the Yangtze River and the Yellow River [*Yang et al.*, 2004] are much weaker (Figures 8a and 8b).

[28] The variability of chemical weathering intensity determines the mineral characteristics of river samples, because coarse and fine grain river sediments must have resulted from different weathering processes. Coarse and quartz rich sediments tend to have lower $Al_2O_3$ values whereas fine grain and clay rich sediments have higher $Al_2O_3$ values. Our major element results show a negative correlation between $SiO_2$ and $Al_2O_3$, suggesting grain-size control on $SiO_2$ content (Figure 4). However, such mineralogical control appears to have had little effect on the chemical weathering intensity of fine grain aluminosilicate minerals from the three river basins. All samples used in this study are argillaceous sediments almost without particles >63 $\mu$m and they were wet sieved (<63 $\mu$m) to reduce any

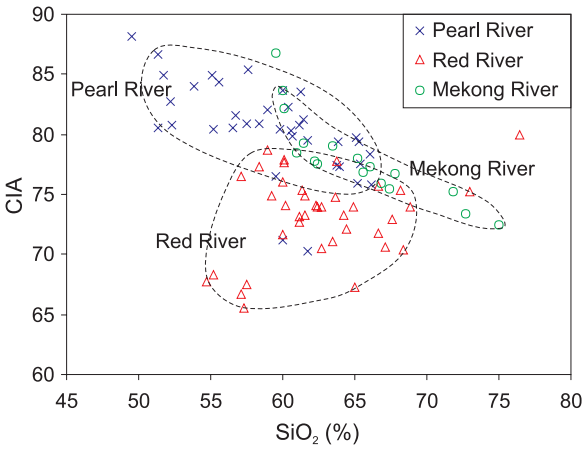


**Figure 9.** Correlation of $SiO_2$ (%) with CIA in argillaceous sediments from the Pearl, Red, and Mekong river basins.

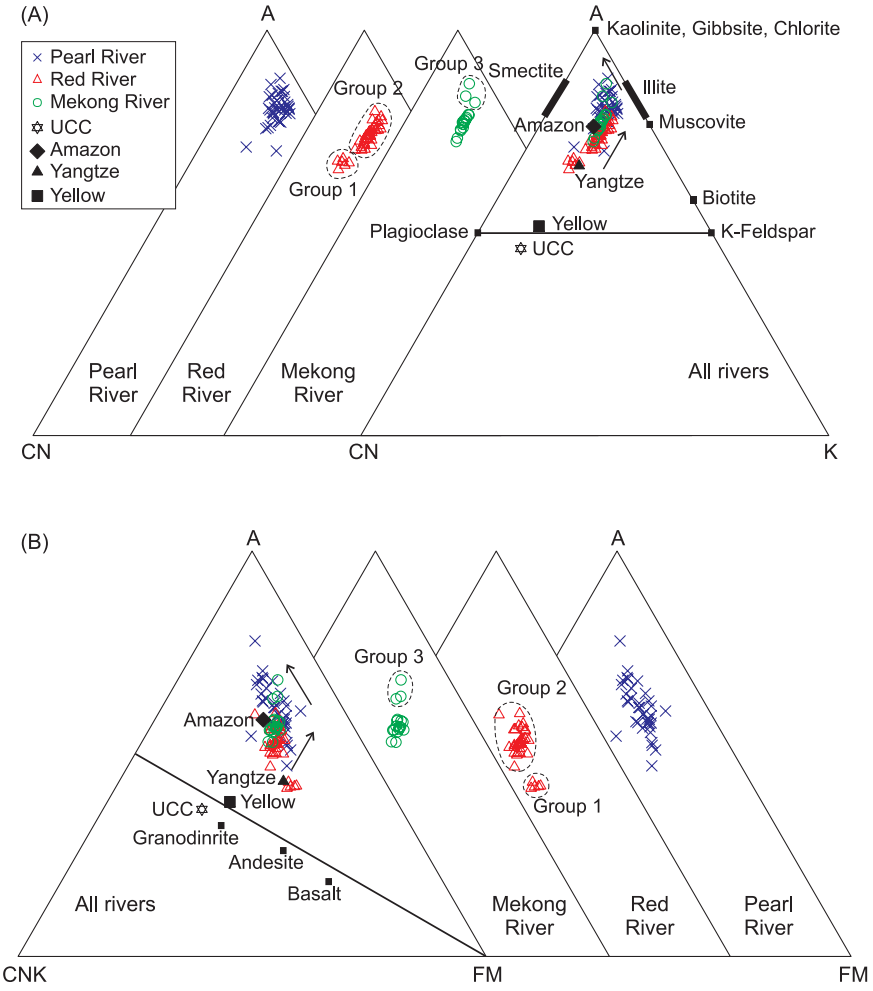


**Figure 10.** (a) A-CN-K and (b) A-CNK-FM ternary diagrams of argillaceous sediments from each of the Pearl, Red, and Mekong river basins and their comparisons. Average data of clayey sediments from the Amazon River [*Vital and Stattegger*, 2000], the Yellow River, and the Yangtze River [*Yang et al.*, 2004] were plotted for comparison; UCC was also plotted as a reference. Arrows indicate predicted weathering trends exhibited by these river sediments, which had experienced intensive weathering for those from the Pearl, moderate weathering for those from the Red, and moderate to intensive weathering for those from the Mekong. The Red River samples in Groups 1 and 2 indicate their sources from intermediate-basic and commonly unweathered rocks, respectively. The Mekong River samples in Group 3 have the same weathering degree as those from the Pearl River. A, $Al_2O_3$; C, CaO; N, $Na_2O$; K, $K_2O$; F, total Fe; M, MgO.

potential grain size effect. Moreover, CIA is a molar ratio of $Al_2O_3/(Al_2O_3 + CaO^* + Na_2O + K_2O)$, which has reduced dilution effects by $SiO_2$ content. The scatterplot of $SiO_2$ versus CIA indicates almost no or weak mineralogical dependence of CIA for the Red and Pearl basins but a clear linear relationship between $SiO_2$ content and the weathering index for the Mekong River basin (Figure 9). Such negative correlation of CIA with $SiO_2$ content in Mekong River samples cannot be explained as the quartz control on CIA, because CIA is independent from $SiO_2$ content. The various CIA values in Mekong River samples are resulted from differently weathered provenances, and most CIA values falling at 75–78 are obviously lower than those of Pearl River samples and higher than those of Red River samples.

[29] Weathering trends in sediments from the Pearl, Red, and Mekong river basins can be clearly observed on $Al_2O_3 - (CaO + Na_2O) - K_2O$ (A-CN-K) and $Al_2O_3 - (CaO + Na_2O + K_2O) - (FeO + MgO)$ (A-CNK-FM) ternary diagrams [*Nesbitt and Young*, 1984, 1989] (Figure 10). The Pearl River sediment samples are plotted closer to the $Al_2O_3$ apex. The Red River sediments can be divided into two parts:

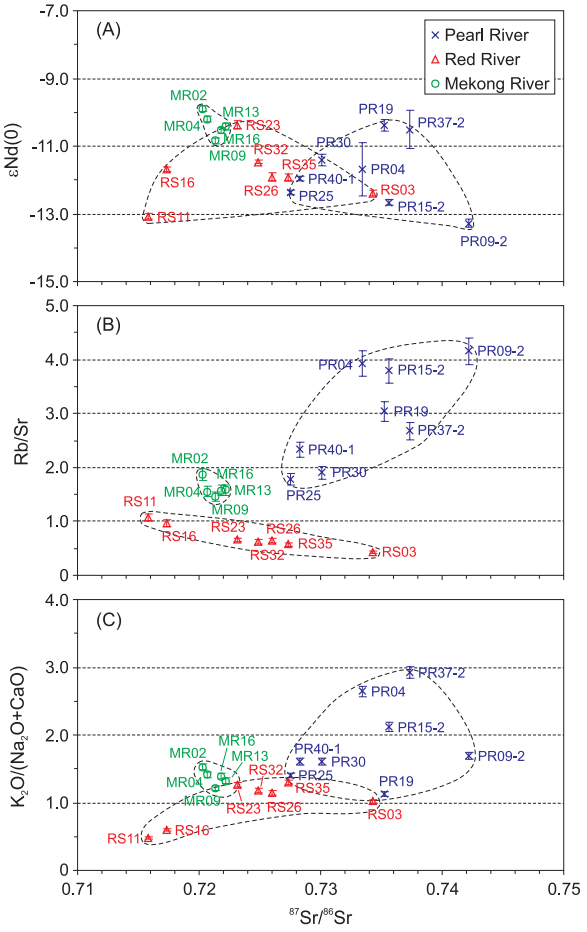


**Figure 11.** Correlations of $^{87}Sr/^{86}Sr$ with (a) $\varepsilon$Nd(0), (b) Rb/Sr, and (c) $K_2O/(Na_2O + CaO)$ molar ratio, indicating the isotopic distribution in argillaceous sediments from the Pearl, Red, and Mekong basins. Error bars refer to the measurement uncertainty. Sample numbers are also marked (see sample locations in Figure 3).

the first six samples (Group 1 in Figure 10) are closer to UCC, indicating more intermediate to basic rock sources; other samples (Group 2 in Figure 10) with higher $Al_2O_3$ are arranged almost parallel to the A-CN line, suggesting a similar composition of unweathered rocks in these samples. While most samples are packed into a field similar to the majority from the Red River, the last three samples (Group 3 in Figure 10) from the Mekong River much closer to the $Al_2O_3$ apex may indicate a weathering degree comparable to those from the Pearl River. The main trends of silicate weathering in all the three river basins display preferential leaching of CaO and $Na_2O$ and enrichment of $Al_2O_3$, while $K_2O$ contents are constant for all sediments from the Red River and for sediments of intermediate weathering stages from the Pearl and Mekong rivers. During strong weathering, leaching of $K_2O$ occurs for most of samples from the Pearl River and the last three samples (Group 3) from the Mekong River. Accordingly, we infer that plagioclase is selectively weathered first in all three river basins, while K-feldspar remains almost intact for all samples from the Red River, most samples from the Mekong River, and a few samples from the Pearl River. These weathering processes have been investigated and confirmed under both experimental and field conditions [*White and Brantley*, 2003]. The leaching of CaO and $Na_2O$ in Yellow and Yangtze river sediments indicates early to intermediate weathering stages [*Yang et al.*, 2004], and the considerable leaching of $K_2O$ in the lowermost Amazon River sediments implies an intensive weathering stage [*Vital and Stattegger*, 2000] (Figure 10). By comparison, silicate weathering can be considered as of moderate for the Red River sediments, moderate to intensive for the Mekong River sediments, and intensive for the Pearl River sediments.

[30] The weathering intensity often influences the Sr isotopic composition in river sediments. On the contrary, neither chemical weathering on land [*Borg and Banner*, 1996] nor grain-size sorting during transport [*Tütken et al.*, 2002; *Goldstein and Jacobsen*, 1988] can significantly modify $\varepsilon$Nd(0) values in sediments subsequently deposited in river basins. The confinement of all $\varepsilon$Nd(0) values from the three studied rivers to a narrow range also conveys a similar message (Figure 11a). Because all the Mekong samples come from the delta downstream and features of their isotopically distinct sources (if there are any) must have been mixed during the confluence, their Nd isotope range considerably narrower than those from the Pearl and the Red is thus reasonable. As they are independent from the weathering process, these $\varepsilon$Nd(0) values can be used as a reference to petrological settings. For each individual river, no relationship between the $\varepsilon$Nd(0) values and the $^{87}Sr/^{86}Sr$ ratios has been observed, suggesting that variations in Sr isotopic composition are not caused by major changes in the petrological source (e.g., basalt). A good correlation between $^{87}Sr/^{86}Sr$ with Rb/Sr ratio and $K_2O/(Na_2O + CaO)$ molar ratio for the three rivers (Figures 11b and 11c), however, denotes a major control on the $^{87}Sr/^{86}Sr$ ratio by Rb/Sr and mineralogical composition in the sediments. High $^{87}Sr/^{86}Sr$ ratios are associated to high $K_2O/(Na_2O + CaO)$ molar ratios, implying the presence of high-Rb, low-Sr minerals such as potassium feldspar and biotite in the river sedi-

ments. In contrast, low $^{87}Sr/^{86}Sr$ ratios are associated to low $K_2O/(Na_2O + CaO)$ molar ratios, implying the presence of low-Rb, high-Sr minerals such as plagioclase (rich in Na and Ca). As the Sr concentration in plagioclase is about 10 times higher than biotite, a low proportion of this mineral can strongly decrease the $^{87}Sr/^{86}Sr$ ratios of the river sediments. Because the $K_2O/(Na_2O + CaO)$ molar ratio is also correlated to other indices of chemical weathering (mineralogical proxies and CIA), we suggest that $^{87}Sr/^{86}Sr$ ratios in river sediments are likely mainly controlled by the state of chemical weathering but not by the presence of basic rocks (such as in the Mekong and the Red rivers). Strong physical erosion in the Red River and in a less extension of the Mekong River would produce sediments with high contents of unaltered plagioclase that induce the nonradiogenic Sr composition.

### 5.3. Climatic Versus Tectonic Controls on Weathering

[31] Climate is an important variable that controls the geochemical environment of weathering processes and also has an overriding influence upon the characteristic of the weathering products [*Nesbitt et al.*, 1980; *McLennan*, 1993; *Gaillardet et al.*, 1999; *Singh et al.*, 2005]. The degree of weathering increases with high mean annual temperature and precipitation. Temperature controls the rate of chemical weathering reactions, and precipitation provides an aqueous medium and moisture for ion exchange for these reactions. Weathering intensity is also related closely to vegetation and runoff, because vegetation keeps moisture for chemical reactions while runoff affects the rates of both chemical and mechanical denudations [*Summerfield and Hulton*, 1994]. All our three river basins mainly experience a humid subtropical East Asian monsoon climate with heavy monsoon precipitation and warm temperature during summers (Figure 2). They are well vegetated through all seasons except the highlands of the Red and Mekong river basins during winter. The annual runoff ranging from 595–1025 mm does not present a significant difference between the basins [*Milliman and Meade*, 1983]. Thus the similar subtropical East Asian monsoon climate along with similar hydrologic conditions should produce a comparable intensity of the chemical weathering in these basins. But on the basis of our results from clay mineralogy and major element geochemistry of surface sediments, the Pearl River basin has a stronger weathering intensity than the Red and Mekong basins. Therefore, beside the monsoon climate, other factors may also control the continental weathering and erosion in the Red and Mekong river basins.

[32] Glacial scour is potentially responsible of stronger physical erosion in the highland part of the Red and Mekong river basins. *Colin et al.* [2006] implied that physical erosion of the highland Himalayas and Indo-Burman Ranges during glacial periods could have been induced by glacial scour and frost action. However, in the central and eastern Tibetan Plateau, where the highland Red and Mekong river basins are located, significant glacial events are absent from the entire Holocene [*Schäfer et al.*, 2002], excluding the glacial scour as a major factor that affects on the physical erosion. Tectonic processes can increase the exposure of fresh, unaltered rock surfaces. The high rates of such physical weathering caused by modern or recent tectonic activities in the eastern Tibetan Plateau and along the Red River fault system [*Replumaz et al.*, 2001; *Schoenbohm et al.*, 2004, 2006a] can produce primary minerals (micas, illite, plagioclase, and K-feldspar). Moreover, the reconstruction of the paleo-Red River indicates ~1400 m river incision and 1400–1500 m surface uplift since the Pliocene [*Schoenbohm et al.*, 2004, 2006b]. Such strong incision produces a suspended sediment yield of 1083 $t/km^2/yr$ for the Red River, about 7 times higher than the Pearl River (157 $t/km^2/yr$) and 5 times higher than the Mekong River (203 $t/km^2/yr$) [*Milliman and Meade*, 1983]. In this way, the tectonic uplift has dramatically increased the slope of the eastern Tibetan margin, where reside the upper to middle reaches of the Red and Mekong rivers. The basin slope is most strongly associated with both mechanical and chemical denudation rates [*Summerfield and Hulton*, 1994]. Therefore more primary minerals formed in the Red and Mekong river basins can indicate more physical erosion than in the Pearl River. These minerals are transported very rapidly to the river delta without chemical alteration. Therefore minerals very sensitive to chemical weathering such as plagioclase are present in the lowlands of the Red and Mekong river sediments.

## 6. Conclusions

[33] The three of the world's largest river basins, the Pearl, Red, and Mekong river basins exhibit different degrees of chemical weathering despite the fact that they are all influenced by East Asian monsoon climate and similar hydrologic condi-

tions. Clay mineralogical indicators (kaolinite/illite ratio, illite chemistry index, and illite crystallinity) and major elemental indexes (chemical mobility, $K_2O/(Na_2O + CaO)$ molar ratio, CIA index, and weathering trend ternary diagrams), combined with Rb, Sr, and Nd concentration and Sr-Nd isotopic results, indicate intensive silicate weathering in the Pearl River basin, moderate to intensive in the Mekong River basin, and moderate in the Red River basin. Our results exclude the parent lithology as a major control on the mineralogical and geochemical compositions of river bed sediments. We suggest that the monsoon climate with heavy precipitation and warm temperature during summers is one of the most significant factors that control the silicate chemical weathering in these three river basins. However, strong physical erosion caused by tectonic activities and river incision in the eastern Tibetan Plateau and along the Red River fault system appears to be responsible for high contents of primary minerals in the lowlands of the Red and Mekong river basins. Although a significant modification of the $\varepsilon$Nd(0) values in our riverine sediments during chemical weathering and transport is unlikely, the $^{87}Sr/^{86}Sr$ ratios are controlled mainly by the state of chemical weathering of high-Sr minerals such as plagioclase (rich in Na and Ca) with a linear decrease trend from the Pearl, Mekong, to Red River basins. Apparently, both climatic and tectonic factors exert control on the present weathering in south China and Indochina Peninsula, contributing to the mineralogical, elemental and isotopic variations in sediments from their rivers.

## Acknowledgments

[34] We thank Tonghua Li, An H. Le, and Nam Phong Le for assistance during fieldworks and Lianwen Liu, Shaoyong Jiang, Lei Shao, and Peijun Qiao for technical help in laboratories. We specially thank Peter D. Clift, Laurent D. Labeyrie, and an anonymous reviewer for their constructive reviews on the early version of this paper. This study was supported by the Natural Science Foundation of China (40331002, 40321603, and 40506014), the Fok Ying Tung Education Foundation (101018), the Doctoral Program of Higher Education (20060247032), the Excellent Young Teachers Program and the Program for New Century Excellent Talents in University of the Ministry of Education of China (NCET-04-0372), and the Laboratory of Marginal Sea Geology Grant of the Chinese Academy of Sciences (BYH03A08).

## References

Borg, L. E., and J. L. Banner (1996), Neodymium and strontium isotopic constraints on soil sources in Barbados, West Indies, *Geochim. Cosmochim. Acta*, *60*, 4193–4206.

Boulay, S., C. Colin, A. Trentesaux, N. Frank, and Z. Liu (2005), Sediment sources and East Asian monsoon intensity over the last 450 kyr: Mineralogical and geochemical investigations on South China Sea sediment, *Palaeogeogr. Palaeoclimatol. Palaeoecol.*, *228*, 250–277.

Burbank, D. W., A. E. Blythe, J. Putkonen, B. Pratt-Sitaula, E. Gabet, M. Oskin, A. Barros, and T. P. Ojha (2003), Decoupling of erosion and precipitation in the Himalayas, *Nature*, *426*, 652–655.

Canfield, D. E. (1997), The geochemistry of river particulates from the continental USA: Major elements, *Geochim. Cosmochim. Acta*, *61*, 3349–3365.

Chamley, H. (1989), *Clay Sedimentology*, 623 pp., Springer, New York.

Chen, P.-Y. (1978), Minerals in bottom sediments of the South China Sea, *Geol. Soc. Am. Bull.*, *89*, 211–222.

Clark, M. K., L. M. Schoenbohm, L. H. Royden, K. X. Whipple, B. C. Burchfiel, X. Zhang, W. Tang, E. Wang, and L. Chen (2004), Surface uplift, tectonics, and erosion of eastern Tibet from large-scale drainage patterns, *Tectonics*, *23*, TC1006, doi:10.1029/2002TC001402.

Clift, P. D. (2006), Controls on the erosion of Cenozoic Asia and the flux of clastic sediment to the ocean, *Earth Planet. Sci. Lett.*, *241*, 571–580.

Clift, P. D., G. D. Layne, and J. Blusztajn (2004), Marine sedimentary evidence for monsoon strengthening, Tibetan uplift and drainage evolution in East Asian, in *Continent-Ocean Interactions Within East Asian Marginal Seas*, *Geophys. Monogr. Ser.*, vol. 149, edited by P. Clift et al., pp. 255–282, AGU, Washington, D. C.

Clift, P. D., A. Carter, I. H. Campbell, M. S. Pringle, N. Van Lap, C. M. Allen, K. V. Hodges, and M. T. Tan (2006a), Thermochronology of mineral grains in the Red and Mekong rivers, Vietnam: Provenance and exhumation implications for Southeast Asia, *Geochem. Geophys. Geosyst.*, *7*, Q10005, doi:10.1029/2006GC001336.

Clift, P. D., J. Blusztajn, and A. D. Nguyen (2006b), Large-scale drainage capture and surface uplift in eastern Tibet–SW China before 24 Ma inferred from sediments of the Hanoi basin, Vietnam, *Geophys. Res. Lett.*, *33*, L19403, doi:10.1029/2006GL027772.

Colin, C., L. Turpin, D. Blamart, N. Frank, C. Kissel, and S. Duchamp (2006), Evolution of weathering patterns in the Indo-Burman Ranges over the last 280 kyr: Effects of sediment provenance on $^{87}Sr/^{86}Sr$ ratios tracer, *Geochem. Geophys. Geosyst.*, *7*, Q03007, doi:10.1029/2005GC000962.

Commission for the Geological Map of the World (1975), *Geological World Atlas*, scale 1:10000000, U. N. Educ. Sci. and Cult. Org., Paris.

Dadson, S. J., et al. (2003), Links between erosion, runoff variability and seismicity in the Taiwan orogen, *Nature*, *426*, 648–651.

Esquevin, J. (1969), Influence de la composition chimique des illites surcristallinite, *Bull. Cent. Rech. Rau SNPA*, *3*, 147–153.

Gaillardet, J., B. Dupre, P. Louvat, and C. J. Allègre (1999), Global silicate weathering and $CO_2$ consumption rates deduced from the chemistry of large rivers, *Chem. Geol.*, *159*, 3–30.

Galy, A., and C. France-Lanord (1999), Weathering processes in the Ganges-Brahmaputra basin and the riverine alkalinity budget, *Chem. Geol.*, *159*, 31–60.

Gingele, F. X., P. D. Deckker, and C.-D. Hillenbrand (2001), Clay mineral distribution in surface sediments between Indonesia and NW Australia: Source and transport by ocean currents, *Mar. Geol.*, *179*, 135–146.

Goldstein, S. J., and S. B. Jacobsen (1988), Nd and Sr isotopic systematic of river water suspended material: Implications for crustal evolution, *Earth Planet. Sci. Lett.*, *87*, 215–221.

Griffin, J. J., H. Windom, and E. D. Goldberg (1968), The distribution of clay minerals in the world ocean, *Deep Sea Res.*, *15*, 433–459.

Gupta, A., L. Hock, X. Huang, and P. Chen (2002), Evaluation of part of the Mekong River using satellite imagery, *Geomorphology*, *44*, 221–239.

Holtzapffel, T. (1985), Les mineraux argileux: Préparation, analyse diffractometrique et determination, *Soc. Geol. Nord Publ.*, *12*, 136 pp.

Jacobsen, S. B., and G. J. Wasserburg (1980), Sm-Nd isotopic evolution of chondrites, *Earth Planet. Sci. Lett.*, *50*, 139–155.

Krumm, S., and W. Buggisch (1991), Sample preparation effects on illite crystallinity measurements: Grain size gradation and particle orientation, *J. Metamorph. Geol.*, *9*, 671–677.

Leloup, P. H., N. Arnaud, R. Lacassin, J. R. Kienast, T. M. Harrison, P. Trinh, A. Replumaz, and P. Tapponnier (2001), New constraints on the structure, thermochronology, and timing of the Ailao Shan-Red River shear zone, SE Asia, *J. Geophys. Res.*, *106*, 6683–6732.

Liu, Z., C. Wang, A. Trentesaux, X. Zhao, H. Yi, X. Hu, and W. Jin (2003), Paleoclimate changes during early Oligocene in the Hoh Xil region, northern Tibetan Plateau, *Acta Geol. Sin.*, *77*, 504–513.

Liu, Z., C. Colin, A. Trentesaux, D. Blamart, F. Bassinot, G. Siani, and M.-A. Sicre (2004), Erosional history of the eastern Tibetan Plateau over the past 190 kyr: Clay mineralogical and geochemical investigations from the southwestern South China Sea, *Mar. Geol.*, *209*, 1–18.

Liu, Z., C. Colin, A. Trentesaux, G. Siani, N. Frank, D. Blamart, and S. Farid (2005), Late Quaternary climatic control on erosion and weathering in the eastern Tibetan Plateau and the Mekong basin, *Quat. Res.*, *63*, 316–328.

McLennan, S. M. (1993), Weathering and global denudation, *J. Geol.*, *101*, 295–303.

Milliman, J. D., and R. H. Meade (1983), World-wide delivery of river sediment to the oceans, *J. Geol.*, *91*, 1–21.

Milliman, J. D., and J. P. M. Syvitski (1992), Geomorphic/tectonic control of sediment discharge to the ocean: The importance of small mountainous rivers, *J. Geol.*, *100*, 525–544.

Molnar, P. (2004), Late Cenozoic increase in accumulation rates of terrestrial sediment: How might climate change have affected erosion rates?, *Annu. Rev. Earth Planet. Sci.*, *32*, 67–89.

Nesbitt, H. W., and G. M. Young (1982), Early Proterozoic climates and plate motions inferred from major element chemistry of lutites, *Nature*, *299*, 715–717.

Nesbitt, H. W., and G. M. Young (1984), Prediction of some weathering trends of plutonic and volcanic rocks based on thermodynamic and kinetic considerations, *Geochim. Cosmochim. Acta*, *48*, 1523–1534.

Nesbitt, H. W., and G. M. Young (1989), Formation and diagenesis of weathering profiles, *J. Geol.*, *97*, 129–147.

Nesbitt, H. W., G. Mackovics, and R. C. Price (1980), Chemical processes affecting alkalis and alkaline Earth during continental weathering, *Geochim. Cosmochim. Acta*, *44*, 1659–1666.

Pédro, G. (1981), Les grands traits de l'évolution cristallochimique des minéraux au cours de l'altération superficielle des roches, *Rend. Soc. Ital. Mineral. Petrol.*, *37*, 633–666.

Pu, W., J. Gao, K. Zhao, H. Ling, and S. Jiang (2005), Separation method of Rb-Sr, Sm-Nd using DCTA and HIBA (in Chinese with English abstract), *Nat. Sci.*, *41*, 445–450.

Raymo, M. E., and W. F. Ruddiman (1992), Tectonic forcing of the late Cenozoic climate, *Nature*, *359*, 117–122.

Raymo, M. E., W. F. Ruddiman, and P. Froelich (1988), Influence of late Cenozoic mountain building on ocean geochemical cycles, *Geology*, *16*, 649–653.

Reiners, P. W., T. A. Ehlers, S. G. Mitchell, and D. R. Montgomery (2003), Coupled spatial variations in precipitation and long-term erosion rates across the Washington Cascades, *Nature*, *426*, 645–647.

Replumaz, A., R. Lacassin, P. Tapponnier, and P. H. Leloup (2001), Large river offsets and Plio-Quaternary dextral strike-slip rate on the Red River fault (Yunnan, China), *J. Geophys. Res.*, *106*, 819–836.

Schäfer, J. M., S. Tschudi, Z. Zhao, X. Wu, S. Ivy-Ochs, R. Wieler, H. Baur, P. W. Kubik, and C. Schlüchter (2002), The limited influence of glaciations in Tibet on global climate over the last 170000 yr, *Earth Planet. Sci. Lett.*, *194*, 287–297.

Schoenbohm, L. M., K. X. Whipple, B. C. Burchfiel, and L. Chen (2004), Geomorphic constraints on surface uplift, exhumation, and plateau growth in the Red River region, Yunnan Province, China, *Geol. Soc. Am. Bull.*, *116*, 895–909.

Schoenbohm, L. M., B. C. Burchfiel, L. Chen, and J. Yin (2006a), Miocene to present activity along the Red River fault, China, in the context of continental extrusion, upper-crustal rotation, and lower-crustal flow, *Geol. Soc. Am. Bull.*, *118*, 672–688.

Schoenbohm, L. M., B. C. Burchfiel, and L. Chen (2006b), Propagation of surface uplift, lower crustal flow, and Cenozoic tectonics of the southeast margin of the Tibetan Plateau, *Geology*, *34*, 813–816.

Ségalen, P. (1995), *Les Sols Ferrallitiques et Leur Répartition Géographique,* vol. 3, *Les Sols Ferrallitiques en Afrique et en Extrême-Orient, Australie, Océanie*, 201 pp., Inst. de Rech. Pour le Dév., Paris.

Selvaraj, K., and C.-T. A. Chen (2006), Moderate chemical weathering of subtropical Taiwan: Constraints from solid-phase geochemistry of sediments and sedimentary rocks, *J. Geol.*, *114*, 101–116.

Singh, M., M. Sharma, and H. J. Tobschall (2005), Weathering of the Ganga alluvial plain, northern India: Implications from fluvial geochemistry of the Gomati River, *Appl. Geochim.*, *20*, 1–21.

Summerfield, M. A., and N. J. Hulton (1994), Natural controls of fluvial denudation rates in major world drainage basins, *J. Geophys. Res.*, *99*, 13,871–13,883.

Taylor, S. R., and S. M. McLennan (1985), *The Continental Crust: Its Composition and Evolution*, 312 pp., Blackwell, Malden, Mass.

Tütken, T., A. Eisenhauer, B. Wiegand, and B. T. Hansen (2002), Glacial-interglacial cycles in Sr and Nd isotopic composition of Arctic marine sediments triggered by the Svalbard/Barents Sea ice sheet, *Mar. Geol.*, *182*, 351–372.

Vital, H., and K. Stattegger (2000), Major and trace elements of stream sediments from the lowermost Amazon River, *Chem. Geol.*, *168*, 151–168.

Wang, P. (2004), Cenozoic deformation and the history of sea-land interactions in Asia, in *Continent-Ocean Interactions Within East Asian Marginal Seas*, *Geophys. Monogr. Ser.*, vol. 149, edited by P. Clift, pp. 1–22, AGU, Washington, D. C.

White, A. F., and S. L. Brantley (2003), The effect of time on the weathering of silicate minerals: Why do weathering rates

differ in the laboratory and field?, *Chem. Geol.*, *202*, 479–506.

Yang, S., H.-S. Jung, and C. Li (2004), Two unique weathering regimes in the Changjjiang and Huanghe drainage basins eochemical evidence from river sediments, *Sediment. Geol.*, *164*, 19–34.

Zhang, C., and L. Wang (2001), Multi-element geochemistry of sediments from the Pearl River system, China, *Appl. Geochem.*, *16*, 1251–1259.

Zhang, J., W. W. Huang, M. G. Liu, and Q. Zhou (1990), Drainage basin weathering and major element transportation of two large Chinese rivers (Huanghe and Changjiang), *J. Geophys. Res.*, *95*, 13,277–13,288.

Zhang, P., P. Molnar, and W. R. Downs (2001), Increased sedimentation rates and grain sizes 2–4 Myr ago due to the influence of climate change on erosion rates, *Nature*, *410*, 891–897.